Homogeneously precessing domains in ^{3}He–B

Yu. M. Bunkov and G. E. Volovik

Kapitsa Institute for Physical Problems, Moscow, Russia
Landau Institute for Theoretical Physics, Moscow, Russia
Centre de Recherches sur les Tres Basses Temperatures, CNRS, Grenoble, France
(Submitted 21 December 1992)
Zh. Eksp. Teor. Fiz. **103**, 1619–1632 (May 1993)

Two different types of homogeneously precessing domains (HPDs) are discussed for ^{3}He–B. In addition to the HPD discovered in 1984, HPD$^{(1)}$, in which the orbital vector is oriented along the magnetic field, another coherently precessing state, HPD$^{(2)}$, is found which is also stable under spatially inhomogeneous perturbations. In the HPD$^{(2)}$ the orbital vector has an opposite orientation. The domain boundaries between different precessing states are discussed. At low temperature the excess of the pumped dipole energy leads to spontaneous formation of a texture of two domains precessing with different frequencies. This produces the phase-slip processes on the domain boundary, which thus plays the part of the weak link between HPD$^{(1)}$ and HPD$^{(2)}$. Evolution of the HPD states in an increasing magnetic field, where the superfluid gap becomes anisotropic, is considered.

1. INTRODUCTION

Superfluid ^{3}He is a magnetic superfluid in which the magnetic ordering is provided by the transition to the coherent quantum state with broken spin rotation symmetry. Besides the equilibrium ground state, the magnetic subsystem can be easily transformed to the excited dynamical state corresponding to the Larmor precession of the deflected magnetization around applied magnetic field. It appeared that the magnetic subsystem can preserve its coherent properties in the regime of the Larmor precession. The precession occurs in a single quantum state and the spatial gradients of the precession phase lead to the spin supercurrent. Such spin stiffness results in the high stability of the homogeneous precession: the spin supercurrent and spin-orbital interaction provide the feedback which supports the single frequency of precession for the whole sample even under inhomogeneous external conditions. The Homogeneously Precessing Domain (HPD) has been observed in ^{3}He–B in 1984.[1,2] This discovery extended the applications of the NMR for investigation of the fine properties of ^{3}He–B, such as spin-supercurrent transport of magnetization[3], nonhydrodynamic corrections to the spin transport of the normal component,[4] and ^{3}He–B properties under rotation.[5] As a result of these investigations the spin-supercurrent Josephson phenomena,[6] the spin-current vortex formation,[7] and modes of HPD oscillations[8] have been discovered. In rotating ^{3}He–B the singly quantized mass-current vortex with the nonaxisymmetric core, and new topological hybrid of i) mass vortex, ii) spin disclination, and iii) Maki soliton have been observed,[9] and the anisotropy of the superfluid density, which is induced by the magnetic field, has been measured.[10]

Recent pulsed NMR experiments in ^{3}He–B at low temperature[11] showed diversity of precessing regimes, indicating that precessing states with different dynamical properties can exist in ^{3}He–B.

Here we show theoretically that two different HPD states should exist in ^{3}He–B: In addition to the HPD investigated so far, which we call here HPD$^{(1)}$, another HPD state, HPD$^{(2)}$, is possible. These two HPD's correspond to two different phases of coherent Larmor precession, which have different symmetries. We consider how the HPD$^{(1)}$ and HPD$^{(2)}$ are modified with increase of the magnetic field, when the B-phase is distorted by the field and becomes anisotropic. The domain boundaries between different states of Larmor precession are discussed. We show that HPD$^{(1)}$ and HPD$^{(2)}$ cannot coexist under the equilibrium Larmor precession with single frequency, but can have a contact in the regime with excess of dipole energy. In this case the HPD$^{(1)}$ and HPD$^{(2)}$ precess with different frequencies, and the domain boundary plays the role of the a Josephson junction, where slippage of the precession phase takes place. The connection with experiment[11] is discussed.

2. LARMOR PRECESSION IN THE DEFORMED B-PHASE

In a conventional experimental situation the dipole energy is low compared with the Zeeman energy, so it may be considered as a perturbation. If this spin-orbital coupling is neglected, the general solution for the free precessing state can be obtained by using the Larmor theorem, which states that in a system rotating with the Larmor frequency $\omega_L = \gamma H$ the effect of the magnetic field is completely compensated and the spin rotation symmetry is restored. As a result one can find all the degenerate coherent states of the Larmor precession by applying to some initial state the symmetry operations $SO_3^S \times SO_3^L$, where SO_3^S is the group of spin rotations in the precessing frame and SO_3^L is the group of orbital rotations in the laboratory frame.

If one chooses as the initial state the stationary state with the equilibrium spin density $\vec{S}^{(0)} = \chi(H)\vec{H}$ and with the equilibrium value of the order parameter $A_{\alpha i}^{(0)}$, then the general solution for the free Larmor precession in arbitrary superfluid phase is

$$A_{\alpha i}(t) = O_{\alpha\beta}(\hat{z}, -\omega_L t) R_{\beta\gamma}^{(S)} O_{\gamma\mu}(\hat{z}, \omega_L t) A_{\mu k}^{(0)} R_{ik}^{(L)}, \quad (2.1)$$

 1063-7761/93/050794-08$10.00 © 1993 American Institute of Physics

$$S_\alpha(t)=O_{\alpha\beta}(\hat{z},-\omega_L t)R^{(S)}_{\beta\gamma}O_{\gamma\mu}(\hat{z},\omega_L t)\chi_B H_\mu. \qquad (2.2)$$

Here $R^{(L)}_{ik}$ is the time-independent matrix of orbital rotations SO_3^L in the laboratory frame and $R^{(S)}_{\beta\gamma}$ is the time-independent matrix of spin rotations SO_3^S in the precessing frame, while the time-dependent matrix $O_{\gamma\mu}(\hat{z},\omega_L t)$ of rotation about axis z through an angle $\omega_L t$ describes the transition from the laboratory frame to a rotating one.

The simplest form for the order parameter in the stationary B-phase disturbed by the magnetic field is:

$$A^{(0)}_{\alpha i}=\Delta_{\|}\,\hat{z}_\alpha\hat{z}_i+\Delta_\perp\,(\delta_{\alpha i}-\hat{z}_\alpha\hat{z}_i), \qquad (2.3)$$

where $\Delta_{\|}$ and $\Delta_\perp$ are longitudinal and transverse gaps. The difference between the gaps increases with the field and the B-phase becomes essentially anisotropic near the transition to the A-phase[12]. In Eq. (2.3) the axis of the anisotropy of the gap is chosen along the magnetic field $\mathbf{H}\|\,\hat{z}$. If one represents the $R^{(S)}$ and $R^{(L)}$ matrices in Euler angles:

$$R^{(S)}=R_z(\alpha_1)R_y(\beta)R_z(\gamma_1),$$

$$(R^{(L)})^{-1}=R_z(\gamma_2)R_y(\lambda)R_z(\alpha_2), \qquad (2.4)$$

one obtains the following general form for the order parameter precessing with the Larmor frequency

$$A(t)=R_z(-\omega_L t+\alpha_1)R_y(\beta)R_z(\omega_L t+\gamma_1)A^{(0)}R_z(\gamma_2)R_y(\lambda)R_z(\alpha_2). \qquad (2.5)$$

The spin density transforms under the symmetry operations as

$$\frac{\vec{S}(t)}{S}=R_z(-\omega_L t+\alpha)R_y(\beta)\hat{z}. \qquad (2.6)$$

The latter means that α is the phase of the precession while β is the tipping angle of the precessing magnetization. The axis of the gap anisotropy is oriented along the vector $\hat{l}=R^{(L)}\hat{z}$, which means that λ and α_2 are polar and azimuthal angles of the orbital anisotropy vector $\hat{l}$. Beside these four variables which describe the orientations of the spin in the precessing frame and the orbital vector in the laboratory frame, there are two more variables: γ_1 and γ_2, but the order parameter depends on them only in combination $\gamma_1+\gamma_2$. So the degenerate states of the Larmor precession in the general case of the B-phase in an arbitrary magnetic field span the 5-dimensional space: $SO_3^S\times SO_3^L$ space of matrices $R^{(S)}$ and $R^{(L)}$ factorized by the space spanned by the residual symmetry operation, which is a simultaneous change of parameters γ, with $\gamma_1+\gamma_2$ fixed.

3. INTERACTIONS WHICH LIFT THE DEGENERACY

The 5-dimensional degeneracy of the Larmor precession is lifted by the dipole interaction averaged over the period of precession

$$F_D=\frac{1}{15}\chi(0)\,\frac{\Omega_L^2}{\Delta_0^2}\,[\langle(TrA)^2\rangle+\langle Tr(A^2)\rangle], \qquad (3.1)$$

where Δ_0 is the isotropic gap in zero field and Ω_L is the longitudinal resonance frequency in the isotropic B-phase. Substituting Eq. (2.5) into Eq. (3.1) one obtains that F_D depends on variables $s_z=\cos\beta=S_z/S$, $l_z=\cos\lambda$ and $\Phi=\alpha_1+\gamma_1+\alpha_2+\gamma_2$:

$$F_D(s_z,l_z,\Phi)=\tfrac{2}{15}\chi(0)\Omega_L^2\,\frac{\Delta_\perp^2}{\Delta_0^2}\,\tilde{F}_D(s_z,l_z,\Phi),$$

$$\begin{aligned}\tilde{F}_D(s_z,l_z,\Phi)=&(s_zl_z-\tfrac{1}{2})^2+\tfrac{1}{8}(1-s_z)^2(1-l_z)^2\\&+\tfrac{1}{4}\cos^2\Phi(1+s_z)^2(1+l_z)^2\\&+q\cos\Phi[(1+s_z)(1+l_z)(s_zl_z-)\\&+(1-s_z^2)(1-l_z^2)](q^2-1)s_z^2l_z^2\\&+\tfrac{1}{2}(q^2+1)(1-s_z^2)(1-l_z^2),\end{aligned} \qquad (3.2)$$

where the parameter

$$q=\frac{\Delta_{\|}}{\Delta_\perp} \qquad (3.3)$$

shows the deformation of the gap caused by the magnetic field.

Note that the pure B-phase is obtained as well for $q=1$ as for $q=-1$, in the latter case the change of sign of $\Delta_\perp$ can be compensated by a shift of the angle Φ by π. As a result one should have

$$F_D(s_z,l_z,\Phi,q=1)=F_D(s_z,l_z,\Phi+\pi,q=-1),$$

which is satisfied by Eq. (3.2).

The profile of the potential $\tilde{F}_D$ as function of s_z and l_z (after minimization over Φ) is shown in Figures 1(a–c) for different magnetic fields. This profile determines the properties of both the pulsed and cw NMR in ^{3}He–B. In the case of pulsed NMR the rf pulse produces a homogeneously precessing state with given tipping angle β (or longitudinal magnetization $s_z=\cos\beta$), which is defined by the amplitude and the duration of the pulse. The minimum of the dipole energy at given s_z defines the equilibrium values of the other variables of the precession and the precession frequency $\omega=\omega_L-\partial F_D/\partial S_z$. The magnetic relaxation leads to the slow drift of s_z and other variables towards the stationary state.

In case of cw NMR the formation of the homogeneous precession state has also been observed[13]. In these experiments the frequency ω of the rf field is fixed, while the tipping angle is adjusted in such a way that the rf field becomes at resonance with the precessing state. In this regime the equilibrium magnetization and other variables of precession are determined by minimization of the energy in a frame, rotating with angular velocity ω. It consists of the dipole energy, averaged over the precession period, and the spectroscopic energy term[14]:

$$F_\omega=(\boldsymbol{\omega}-\gamma\mathbf{H})\cdot\mathbf{S}=\frac{\chi(H)}{\gamma^2}\,\omega_L(\omega-\omega_L)s_z. \qquad (3.4)$$

The magnetic relaxation is compensated by the power supply from the rf field.

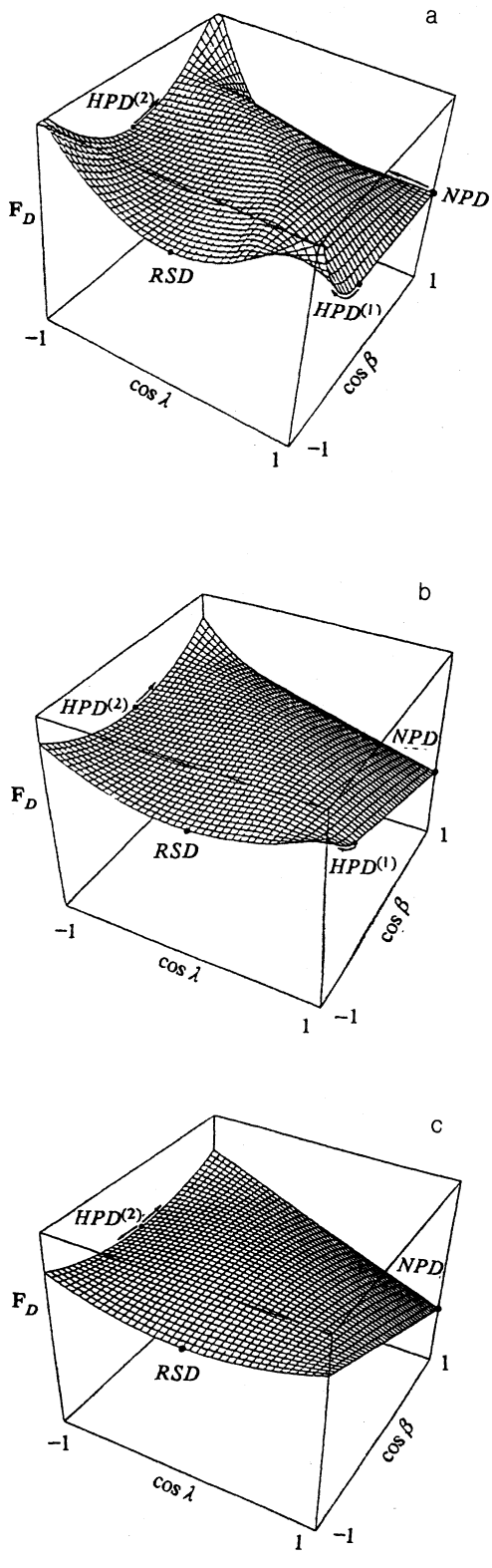

FIG. 1. Profile of dipole energy in ^{3}He–B in terms of the normalized longitudinal magnetization $s_z=\cos\beta$ and orbital angular momentum $l_z=\cos\lambda$ for different gap deformation induced by a magnetic field. a) B-phase in a relatively weak field where the gap deformation can be neglected: $\Delta_\parallel=\Delta_\perp$. Two valleys are seen, which are separated by the energy barrier. The right valley is responsible for the nonprecessing state (NPD) and the conventional HPD$^{(1)}$ with $l_z=1$, while the left one gives rise to the domain with the reversed spin (RSD, $s_z=-1$, $l_z=0$) and to the HPD$^{(2)}$ with the reversed orbital momentum, $l_z=-1$, and $s_z>0$. b) B-phase in such a field that $\Delta_\parallel=0.5\Delta_\perp$. c) The field is so strong that the longitudinal gap disappears, $\Delta_\parallel=0$, and the B-phase transforms to the planar state. HPD$^{(1)}$ does not exist in this state.

4. HPD STATES

The profile of the dipole energy in the B-phase leads to several different coherent states. The right valley of the dipole energy profile on Fig. 1 leads to the following states.

(i) Nonprecessing state (NPD). This is the stationary state with equilibrium magnetization, $s_z=1$. In the pure (nondeformed) B-phase this state is degenerate with respect to the orientation of the orbital angular momentum within the range $-1/4<l_z<1$. The local orientation of the vector l is determined by other perturbations, like surface conditions on the walls, as a result the texture of the vector l appears. For the deformed B-phase the degeneracy is lifted and the minimum of the dipole energy, $\tilde{F}_D^{\rm NPD}=-3/4(1-q^2)$, occurs at $l_z=1$ and $\cos\Phi=-q/4$. The equilibrium value of Φ is the Leggett angle for the deformed B-phase[12].

(ii) The modified Brinkman–Smith (BS) mode. It has $l_z=1$, and

$$\cos\Phi=q\frac{1-2s_z}{2+2s_z}. \tag{4.1}$$

The magnetization should be within the range

$$1>s_z>\frac{q-2}{2q+2}, \tag{4.2}$$

to preserve $\cos\Phi<1$. This solution has a linear dependence of the dipole energy on the longitudinal spin:

$$\tilde{F}_D^{\rm BS}(s_z)-\tilde{F}_D^{\rm NPD}=(1-q^2)(1-s_z). \tag{4.3}$$

This means the following:

a) All the BS states have the same precession frequency $\omega=\omega_L-\partial F_D^{\rm BS}/\partial S_z$ which in dimensional units

$$w=\frac{15\omega_L(\omega-\omega_L)\Delta_0^2}{2\Omega_L^2\Delta_\perp^2} \tag{4.4}$$

is

$$w^{\rm BS}=1-q^2. \tag{4.5}$$

This finite frequency shift coincides with the resonance frequency shift of the transverse linear NMR on the NPD state, since the latter corresponds to the BS mode with small β. In the B-phase the resonance frequency shift of the transverse NMR exists only due to the gap deformation and is known as the g-shift[15]. The g shift was first measured by Osheroff[16] and investigated in detail in [17].

b) In the applied field gradient the BS states are unstable to the phase separation, i.e., to formation of two domains with the magnetizations corresponding to the extreme values in Eq. (4.2). These are the NPD state, which appears in the region of the cell where the local frequency shift is less than $w^{\rm BS}$, and the conventional HPD (HPD$^{(1)}$), which appears in the region of the cell where $w>w^{\rm BS}$.

(iii) HPD$^{(1)}$ state. This state has the same orbital momentum $l_z=1$ as in the BS mode. It is characterized by higher tipping angle:

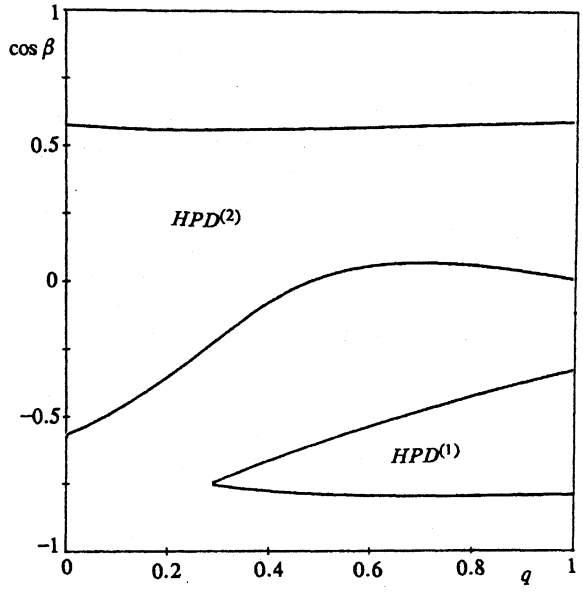

FIG. 2. The stability regions for HPD$^{(1)}$ and HPD$^{(2)}$ for different deformation of the gap, $q=\Delta_{\parallel}/\Delta_{\perp}$. In the planar phase ($q=0$) the conventional HPD (HPD$^{(1)}$) is never stable, while the interval of the tipping angles of the precessing magnetization, in which the HPD$^{(2)}$ is stable, is largest: $|\cos\beta|<1/\sqrt{3}$.

$$\cos\beta=s_z<\frac{q-2}{2q+2} \tag{4.6}$$

and $\cos\Phi=1$. In the free precession after the rf pulse the state with any value of magnetization within this range is stable to phase separation, since the energy in this state

$$\tilde{F}_D^{\mathrm{HPD1}}(s_z)=(1-q)+\left(s_z(1+q)+\frac{1}{2}\right)^2 \tag{4.7}$$

is a concave function of s_z. From Eq. (4.7) one can find the following relation between the magnetization and the resonance frequency of precession in terms of the dimensionless frequency shift w:

$$s_z=-\frac{1}{2(1+q)}-\frac{w}{2(1+q)^2}. \tag{4.8}$$

HPD$^{(1)}$ exists at the frequency shifts $w>w^{\mathrm{BS}}=1-q^2$. On the other hand, at large frequency shift, which corresponds to the large tipping angle β, HPD$^{(1)}$ becomes unstable to deviation of $\hat{l}$ from the field direction (see Fig. 1c). This means that the HPD$^{(1)}$ state never exists (see Fig. 2) for q small enough.

The other states result from the left valley of the dipole energy profile on Fig. 1.

(iv) Reversed Spin Domain (RSD). It has an inverse direction of magnetization, $s_z=-1$, and a transverse orbital momentum, $l_z=0$, while Φ is arbitrary in this domain.[18] The dipole energy of this mode is $\tilde{F}_D^{\mathrm{RSD}}=3/4$. This state cannot be stabilized by a cw rf field: it cannot pump power from the rf field since the transverse magnetization is absent. The decay of this state can occur for example in the following way: The reversed orientation is preserved, while the magnitude of the spin decreases.

(v) HPD$^{(2)}$ state. This is the mode with reversed orbital momentum, $l_z=-1$, and arbitrary Φ.[18,19] Its energy

$$\tilde{F}_D^{\mathrm{HPD2}}(s_z)=\tfrac{3}{4}+(q^2+\tfrac{1}{2})s_z^2 \tag{4.9}$$

is a concave function of s_z, which means that this state is stable to phase separation and thus can homogeneously precess in the cell. The longitudinal magnetization and the normalized frequency shift are coupled by the following relation:

$$s_z=-\frac{w}{1+2q^2}. \tag{4.10}$$

One can see from Fig. 1 that in some region of magnetization HPD$^{(2)}$ is unstable towards the deviation of $\hat{l}$ from its antiparallel orientation. Figure 2 shows the region of stability of HPD$^{(2)}$.

(vi) At small fields when the gap deformation can be neglected there is a mode situated between the RSD and HPD$^{(2)}$.[19] In this state $\cos\Phi=-1$ and l_z changes between 0 and -1 while s_z changes between -1 and 0 according to equation $(1-s_z)(1-l_z)=2$. Its energy, $\tilde{F}_D(s_z)|_{q=1}=3/4$, does not depend on s_z and therefore in a free precession it is separated into RSD and HPD$^{(2)}$. At finite gap deformation this solution disappears and the energy barrier appears between RSD and HPD$^{(2)}$.

It is worth mentioning again that the energy correspond to two different classes of solutions of the Leggett–Takagi equations for the precessing order parameter. The first one is the analytical Brinkman–Smith solution, which corresponds to the walley HPD$^{(1)}$-BS-NPD. The second class of solutions, which correspond[1] to the walley between RSD and HPD, has been recently found in numerical simulations[20].

5. TWO- AND THREE-DOMAIN PRECESSION

In pulsed NMR experiments the total magnetization in the cell is determined by the magnitude and duration of the pulse. In an applied-field gradient the total magnetization is redistributed in the cell to produce one, two, or even three domains of the stable or metastable phases of precession. This is analogous to the separation into a gas and a liquid in the presence of the gravity field. Since there are several phases of the precession (NPD, HPD$^{(1)}$, HPD$^{(2)}$, RSD), the formation of this phase domains is determined by the total magnetization, by the field gradient, and also by the characteristics of the rf pulse. Anyway, in equilibrium the precession frequency ω is constant along the whole sample. This results from the spin stiffness which establishes the coherence of the precession phase α_1. The nonequilibrium situation, when the domains have different frequencies, is discussed in the next section. In the pulsed NMR the magnetic relaxation leads to the slow drift of the domain boundary, while in NMR the two-domain precession is stabilized by the rf field: The frequency of rf field defines the position of the interface and the power supply compensates for the energy dissipation.

Let us now consider which domains can coexist with each other and where is the position of the domain bound-

ary within the cell. The conditions for the coexistence of two precessing states in equilibrium are equivalent to that of the gas-liquid system, and are obtained from the latter by substitution $\mu \to -\omega$, $\rho \to S_z$ (μ is the chemical potential and ρ is the mass density):

$$\omega_1 = \omega_2 = \omega, \tag{5.1a}$$

$$E_1(S_{1z}) + \omega S_{1z} = E_2(S_{2z}) + \omega S_{2z}. \tag{5.1b}$$

This means that the contacting states should have the same precession frequency at the domain boundary and the same potential

$$E(S_z) + \omega S_z = F_D(S_z) + (\omega - \omega_L) S_z,$$

where the energy density $E(S_z)$ includes the Zeeman and the dipole energies. The Eq. (5.1b), which corresponds to the requirement of pressure similarity on both sides of the liquid-gas interface, means that the sum of dipole and spectrosopic energies should be equal on both sides of the interface.

Till now the only two-domains precession which has been discovered[1,2] and intensively exploited is the precession with the NPD and HPD$^{(1)}$ in the cell. From Eqs. (5.1) one finds that the interface between these states should exist in a place of the cell where the frequency of two-domains precession is shifted from the local Larmor frequency $\omega_L(\mathbf{r})$ by the value [in the normalized units of Eq. (4.4)]:

$$w(\mathrm{NPD}-\mathrm{HPD}^{(1)}) = 1 - q^2. \tag{5.2}$$

At low gap deformation where $q \approx 1$ this corresponds to a zero frequency shift.

In principle other pairs of states can coexist. As follows from Eqs. (5.1) the interface between RSD and HPD$^{(1)}$ is positioned in the place where the local frequency shift is

$$w(\mathrm{RSD}-\mathrm{HPD}^{(1)}) = (1+q)(1+2q-\sqrt{2+4q^2}), \tag{5.3}$$

and the interface between RSD and HPD$^{(2)}$ is at the place where $w(\mathrm{RSD}-\mathrm{HPD}^{(2)}) = 0$. For a long enough cell or for a large enough gradient the three-domain precession can take place[18]: RSD–HPD$^{(1)}$–NPD. This can occur if the difference in the local Larmor frequencies between the ends of the cell exceeds $w(\mathrm{RSD}-\mathrm{HPD}^{(1)}) - w(\mathrm{NPD}-\mathrm{HPD}^{(1)}) = (1+q)(3q - \sqrt{2+4q^2})$.

For a weak field, an interface between NPD and RSD is impossible, since it can occur at $\omega = 0$, where the stability of both domains is marginal. At large gap deformation, i.e. at small enough q, an interface between NPD and RSD becomes possible. The frequency shift of the precession with respect to the local Larmor frequency at the position of the interface, which is found from the general conditions (5.1), is

$$w(\mathrm{RSD}-\mathrm{NPD}) = \tfrac{3}{8}(2-q^2). \tag{5.4}$$

To ensure stability of NPD, this frequency shift should be smaller than the frequency shift of BS state, $w^{\mathrm{BS}} = 1 - q^2$. This gives the condition $q < \sqrt{2/5}$, at which the coexistence of these domains can take place. It is worth mentioning that the formation of a dynamical two-domain structure with opposite orientations of the magnetization was proposed to explain the results of the NMR experiments on the spin polarized ^{3}He–^{4}He solution, where the long-lived induction signal has been observed.[21] Since each of two domains has no transverse magnetization, the long-lived signal is assumed to be radiated by the transverse magnetization within the domain boundary, which moves slowly along the cell in the process of the magnetic relaxation.

6. SPONTANEOUS AC JOSEPHSON EFFECT: DOMAIN BOUNDARY AS A WEAK LINK

In the two domain precession the position of the domain boundary in the cell defines both the total spin $\mathbf{S}_z = \int dV S_z$

$$\mathbf{S}_z = V_1 S_{1z} + V_2 S_{2z}, \tag{6.1}$$

and the total energy, $\mathbf{E} = \int dV\ E = \mathbf{F}_D - \omega_L \mathbf{S}_z$

$$\mathbf{E} = V_1 E_1(S_{1z}) + V_2 E_2(S_{2z}), \tag{6.2}$$

of the two-domains precessing state. Here V_1 and V_2 are the volumes of domains, with $V_1 + V_2 = V$ being the total volume, and $\mathbf{F}_D = \int dV\ F_D$ is the total dipole energy of the system. When the domain boundary sweeps the cell the energy $\mathbf{F}_D$ changes as a function of the total magnetization, $\mathbf{F}_D = \mathbf{F}_D^{\mathrm{eq}}(\mathbf{S}_z)$, which is believed to hold for the HPD$^{(1)}$–NPD interface at $T > 0.3T_c$.

However, at low temperature the situation can change. In the pulsed NMR the state that forms just after the rf pulse appears to depend on the starting conditions defined by the texture of the $\hat{l}$ vector. We may suggest that the short but powerful rf pulse deflects the magnetization, preserving the initial local direction of $\hat{l}$. As a result the obtained state has an excess dipole energy compared with the equilibrium energy corresponding to the obtained magnetization: $\mathbf{F}_D > \mathbf{F}_D^{\mathrm{eq}}(\mathbf{S}_z)$. At high temperature the excess of the dipole energy swiftly relaxes due to the Leggett–Takagi dissipation mechanism, but at low temperature the system can live a long time with the excess of the dipole energy. What is the configuration of the precessing state in this regime?

Let us consider for example the case of an HPD$^{(1)}$–NPD interface, for simplicity in the limit of a small gap deformation. The magnetization and the dipole energy of the NPD are fixed, $S_{1z} = S$ and $F_{1D}(S_{1z}) = 0$, while those of the HPD$^{(1)}$ in equilibrium with NPD are $\mathbf{S}_{2z}^{\mathrm{eq}} = -S/4$ and $\mathbf{F}_{2D}^{\mathrm{eq}} = 0$. The total dipole energy for the equilibrium two domain precession is thus zero, $\mathbf{F}_D^{\mathrm{eq}} = 0$. Therefore any nonzero value of the dipole energy, $\mathbf{F}_D \neq 0$, gives an energy excess. Applying Eqs. (6.1) and (6.2) one can find the position of the interface (or the relative volume of one of the domains V_1/V) and the magnetization in the HPD$^{(1)}$ in terms of the energy excess. This gives the following precession frequency of HPD$^{(1)}$

$$\omega(\mathrm{HPD}^{(1)}) = \omega_L + \frac{4}{3}\frac{\Omega_L^2}{\omega_L}\frac{f + \sqrt{2f(1-\bar{s}_z)}}{f + 1 - \bar{s}_z + \sqrt{2f(1-\bar{s}_z)}}, \tag{6.3}$$

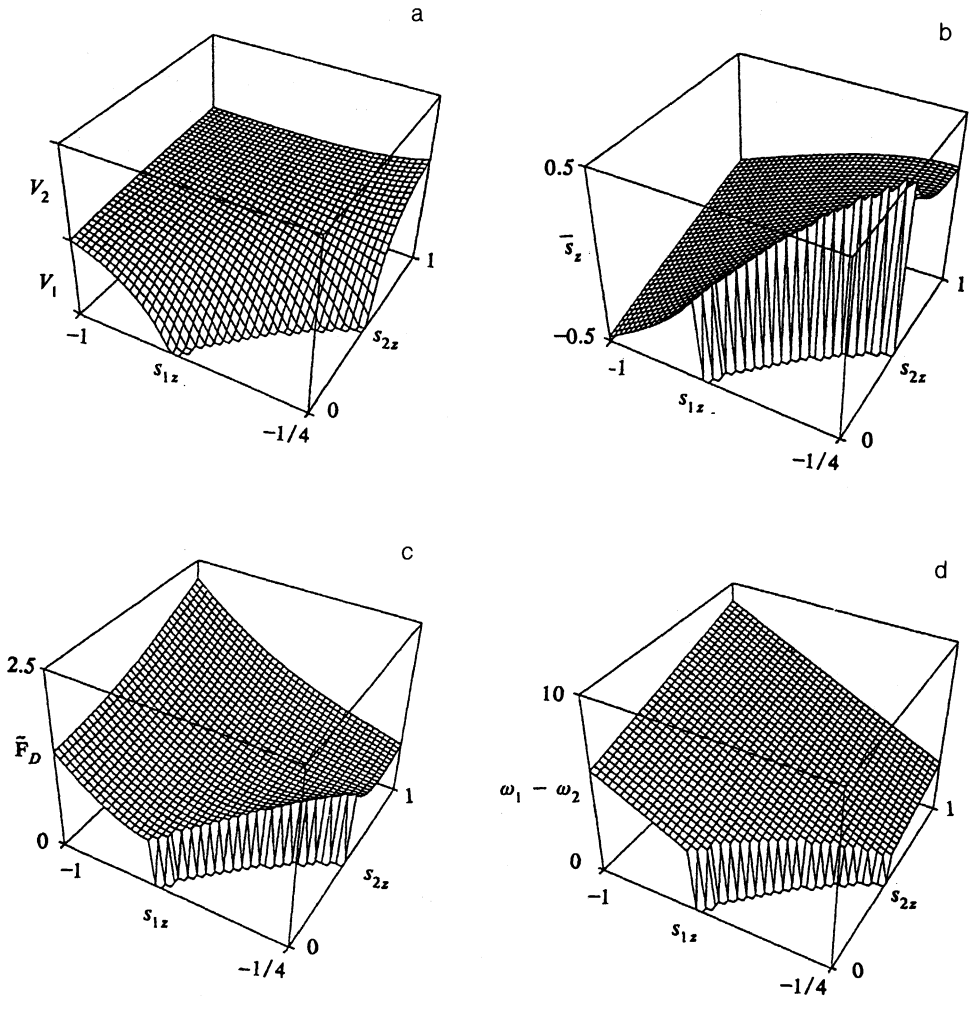

FIG. 3. Coexistence of HPD$^{(1)}$ and HPD$^{(2)}$ in the regime of the energy excess. a) Position of the domain boundary in terms of the normalized longitudinal magnetizations s_{1z} and s_{2z} of coexisting domains. The volume V_1 is occupied by HPD$^{(1)}$, while the rest volume $V_2 = V - V_1$ is occupied by HPD$^{(2)}$. b) Average spin in the cell $\bar{s}_z = (s_{1z}V_1 + s_{2z}V_2)/V$. c) The dipole energy of two-domains texture averaged over the cell, $\tilde{F}_D/V$, in the dimensionless units of Eq. (3.2). d) The jump of the precession frequency, $\omega_1 - \omega_2$, at the HPD$^{(1)}$–HPD$^{(2)}$ interface in the dimensionless units of Eq. (4.4).

where f is a dimensionless parameter related to the total excess of the dipole energy $\mathbf{F}_D = V4/3\chi\Omega_L^2 f$, and $\bar{s}_z$ describes the magnetization averaged over the cell: $\mathbf{S}_z/V = \chi H\bar{s}_z$. It is important that the calculated precession frequency of HPD$^{(1)}$ does not correspond to the frequency ω_L at which there is an equilibrium contact between NPD and HPD$^{(1)}$: $\omega(\text{HPD1}) > \omega_L$, whereas the frequency on the NPD side should be less than ω_L due to the stability requirement.

This means that in the general case of two-domain precession in the regime of the excess of the energy, the two domains have different frequencies, i.e. there is a spontaneous jump of the precession frequencies at the domain boundary. This jump leads to the same *ac* Josephson effect as in the case of the applied voltage across the weak link in superconductors: the phase slippage occurs within the interface, and compensates for the difference in the winding rate of the precession phase α_1 on both sides of the interface. Due to dissipation which accompanies the phase-slip process the excess $\mathbf{F}_D$ of the dipole energy relaxes and the precession frequencies of the domains become equal. After that the conventional equilibrium two-domain precession takes place.

The spontaneous frequency jump, accompanied by the phase slippage on the domain boundary, provides the possibility of coexistence of the domains, which cannot coexist in a conventional equilibrium situation. In particular an HPD$^{(1)}$–HPD$^{(2)}$ interface becomes possible. This situation can occur in pulsed NMR due to the $\hat{l}$ texture which is usually present in the nonprecessing state because of the normal boundary conditions on the $\hat{l}$ vector. If the strong rf field is applied in a short pulse, the $\hat{l}$ texture is not disturbed just after the pulse. As a result the HPD$^{(2)}$ should be formed in the region where $\hat{l}$ essentially deviates from the field direction (near the side walls of the cylindrical vessel), while in the region of small deviation (near the axis of the vessel) the conventional HPD$^{(1)}$ is formed. Further developement depends on the complicated dynamics of the phase-slip boundaries between HPD$^{(1)}$, HPD$^{(2)}$, NPD and RSD.

How to find the position of the interface between two precessing domains and the values of magnetization in the

domains, S_{1z} and S_{2z} in the regime of the energy excess? The Eqs. (6.1) and (6.2) provide only two conditions for three variables, V_1, S_{1z} and S_{2z}. The third equation should be related with the local stability condition for the boundary position. This is Eq. (5.1b), which ensures equal pressure on both sides of the interface, while the Eq. (5.1a) cannot be satisfied in the regime of the energy excess. This just means that the difference in the precession frequency, $\omega_1-\omega_2$, appears across the domain boundary. Consequently the phase slip processes with the period $2\pi/|\omega_1-\omega_2|$ take place. The Lagrange multiplier ω is:

$$\omega=\omega_L-\left.\frac{\partial \mathbf{F}_D}{\partial \mathbf{S}_z}\right|_{\omega_1-\omega_2}, \quad \omega^{\mathrm{HPD2}}<\omega<\omega^{\mathrm{HPD1}}. \tag{6.4}$$

To solve these equations let us invert the problem and minimize the potential $\mathbf{E}+\omega\mathbf{S}_z$ at fixed frequency jump $\omega_1-\omega_2$. In this case one obtains the energy excess in terms of the frequency jump. This corresponds to the physical situation when the frequency jump is supported by the applied rf field in the same manner as rf field supports the voltage in the Josephson junction in superconductors producing the Shapiro steps. The frequency jump should be related to the frequency ω_{rf} of the rf field as $\omega_1-\omega_2=n\omega_{rf}$, with integer n. In the typical experimental situation the applied rf frequency should be ~ 1 kHz which is rather small compared with the precession frequency ~ 1 MHz.

In Fig. 3 we show the position of the $\mathrm{HPD}^{(1)}-\mathrm{HPD}^{(2)}$ interface, the total magnetization and the total energy in terms of the tipping angles of magnetization, s_{1z} and s_{2z}, of $\mathrm{HPD}^{(1)}$ and $\mathrm{HPD}^{(2)}$ coexisting in the regime of the Josephson effect. The region of s_{1z} and s_{2z} where such coexistence is possible is defined by the following relation:

$$s_{2z}>s_{1z}+\sqrt{s_{1z}^2+\tfrac{1}{2}-\tfrac{8}{3}(s_{1z}+\tfrac{1}{4})^2}, \tag{6.5}$$

which should be strengthened by the local stability conditions for $\mathrm{HPD}^{(1)}$ and $\mathrm{HPD}^{(2)}$

$$s_{1c}<s_{1z}<-\tfrac{1}{4}, \quad s_{2c}>s_{2z}>0. \tag{6.6}$$

Here $s_{1c}=-(7+\sqrt{609})/40$ and $s_{2c}=(\sqrt{41}-1)/10$ are critical values at which the deviation of the $\hat{l}$ vector from the parallel orientation in $\mathrm{HPD}^{(1)}$ and from the antiparallel orientation in $\mathrm{HPD}^{(2)}$ becomes energetically favourable.

In the regime of the decay after the rf pulse the total spin and the dipole energy excess are given. They define the magnetizations of domains, s_{1z} and s_{2z}. These are found by intersecting the surfaces on Fig. 3b and Fig. 3c by the planes of constant $\mathbf{S}_z$ and $\mathbf{F}_D$. The interface position and the frequency jump are then determined from Fig. 3a and Fig. 3d. In the process of energy relaxation the two-domains solution vanishes.

If the frequency jump can be stabilized by an rf field with low frequency corresponding to the radiation from the Josephson junction (domain wall), then the total spin and $\omega_1-\omega_2$ are fixed. The magnetizations s_{1z} and s_{2z} are now found by intersecting the surfaces on Fig. 3b and Fig. 3d by the planes of constant $\mathbf{S}_z$ and $\omega_1-\omega_2$. After that the interface position and the dipole energy are obtained from Fig. 3a and Fig. 3c.

7. DISCUSSION

The possibility of the existence of two-domain structure in the regime of an excess of the dipole energy at low temperature agrees qualitatively with the recent experiments made at $T\sim 0.12T_c$.[11] In these experiments, a complicated behavior of the long-lived induction signal was observed. In particular, the observed beating of two frequences at the first stage of free precession can be compared with the different frequencies of the domains, $\mathrm{HPD}^{(1)}$ and $\mathrm{HPD}^{(2)}$, which can coexist in the initial regime of the energy excess. Note that experimentally the signal which survives after the complicated reconstruction at the first stage and lives long in the final stage of precession has the higher frequency. This corresponds in fact to the $\mathrm{HPD}^{(1)}$ which should remain after the relaxation of excess energy. It was also shown that the properties of the signal essentially change from run to run at the same external parameters of NMR (amplitude, frequency, and duration of the rf pulse). This can be related to different textures in the $\hat{l}$ vector before the rf pulse is applied, and therefore to different excesses of the dipole energy over the equilibrium level. The latter should lead to different scenario of the formation of the coherently precessing states and different processes of the relaxation of magnetization, and also to the formation of different $\hat{l}$ textures to the moment of the next exciting pulse.

Although a direct comparison of the theoretical and experimental results on the long-lived signal at low temperatures requires further theoretical and experimental efforts, the qualitative picture of the behavior of the coherent magnetization in the magnetic superfluid seems to be consistent with the experiment. If the interpretation of the first stage of the long-lived iduction signal as the *ac* Josephson effect, spontaneously arising at the interface between two domains, is correct, then one can try to stabilize this regime by application of an rf field whose low frequency ω_{rf} is matched to the frequency difference between the domains according to relation $\omega_1-\omega_2=n\omega_{\mathrm{rf}}$.

We are grateful to I. A. Fomin for illuminating discussions and to the staff of CRTBT-CNRS, where this work has been done, for kind hospitality extended to us.

[1] A. S. Borovik-Romanov, Yu. M. Bunkov, V. V. Dmitriev, and Yu. M. Mukharskiĭ, Pisma Zh. Eksp. Teor. Fiz. **40**, 256 (1984); [JETP Lett. **40**, 1033 (1984)].
[2] I. A. Fomin, Pisma Zh. Eksp. Teor. Fiz. **40**, 260 (1984); [JETP Lett. **40**, 1037 (1984)].
[3] A. S. Borovik-Romanov, Yu. M. Bunkov, V. V. Dmitriev, Yu. M Mukharsky, and D. A. Sergatskov, Phys. Rev. Lett. **62**, 1631 (1989).
[4] Yu. M. Bunkov, V. V. Dmitriev, A. V. Markelov, Yu. M. Mukharskiĭ, and D. Einzel, Phys. Rev. Lett. **65**, 867 (1990).
[5] Yu. M. Bunkov and P. J. Hakonen, J. Low. Temp. Phys. **83**, 323 (1991).
[6] A. S. Borovik-Romanov, Yu. M. Bunkov, A de Waard, V. V. Dmitriev, V. Makrotsieva, Yu. M. Mukharskiĭ, and D. A. Sergatskov, Pisma Zh. Eksp. Teor. Fiz. **47**, 400 (1988); [JETP Lett. **47**, 478 (1988)].
[7] A. S. Borovik-Romanov, Yu. M. Bunkov, V. V. Dmitriev, Yu. M. Mukharskiĭ, and D. A. Sergatskov, Physica B **165**, 649 (1990).

[8] Yu. M. Bunkov, V. V. Dmitriev, and Yu. M. Mukharskiĭ, Physica B **178**, 196 (1992).
[9] Y. Kondo, J. S. Korhonen, M. Krusius, V. V. Dmitriev, Yu. M. Mukharskiĭ, E. B. Sonin, and G. E. Volovik, Phys. Rev. Lett. **67**, 81 (1991); Y. Kondo, J. S. Korhonen, M. Krusius, V. V. Dmitriev, E. V. Thuneberg and G. E. Volovik, Phys. Rev. Lett. **68**, 3331 (1992).
[10] J. S. Korhonen, Yu. M. Bunkov, V. V. Dmitriev, Y. Kondo, M. Krusius, Yu. M. Mukharskiĭ, Ü. Parts, and E. V. Thuneberg, Report TKK-F-A702, Finland, submitted to Phys. Rev. B.
[11] Yu. M. Bunkov, S. N. Fisher, A. M. Guenault, and G. R. Pickett, Phys. Rev. Lett. **69**, 3092 (1992).
[12] N. Schopohl, J. Low Temp. Phys., **49**, 347 (1982).
[13] A. S. Borovik-Romanov, Yu. M. Bunkov, V. V. Dmitriev, Yu. M. Mukharskiĭ, E. V. Poddyakova, and O. D. Timofeevskaya, Zh. Eksp. Teor. Fiz. **96**, 956 (1989); [Sov. Phys. JETP **69**, 542 (1989)].
[14] A. Abragam, and M. Goldman, *Nuclear Magnetism: Order and Disorder*, Clarendon Press, Oxford, 1982.
[15] Y. Hasegava, Prog. Theor. Phys. **70**, 1141 (1983).
[16] D. D. Osheroff, Phys. Rev. Lett. **33**, 1009 (1974).
[17] H. H. Hensley, G. F. Moores, M. R. Rand, T. M. Haard, J. B. Kycia, P. Hamot, Y. Lee, W. P. Halperin, and E. V. Thuneberg, J. Low Temp. Phys. **89**, 505 (1992).
[18] J. S. Korhonen, and G. E. Volovik, Pisma Zh. Eksp. Teor. Fiz. **55**, 358 (1992) [JETP Lett. **55**, 362 (1992)].
[19] G. E. Volovik, submitted to J. Phys.: Cond. Matter.
[20] V. L. Golo and A. A. Leman, Physica B **169**, 525 (1991); J. Low Temp. Phys. **80**, 89 (1990).
[21] G. Nunes Jr., C. Jin, D. L. Hawthorne, A. M. Putnam, and D. M. Lee, Phys. Rev. B **46**, 9082 (1992).

This article was published in English in the original Russian journal. It is reproduced here with the stylistic changes by the Translation Editor.